

## PLANETARY SYSTEMS IN BINARIES. I. DYNAMICAL CLASSIFICATION

GENYA TAKEDA<sup>1</sup>, RYOSUKE KITA<sup>1</sup>, AND FREDERIC A. RASIO<sup>1</sup>

*submitted to ApJ*

### ABSTRACT

Many recent observational studies have concluded that planetary systems commonly exist in multiple-star systems. At least  $\sim 20\%$  of the known extrasolar planetary systems are associated with one or more stellar companions. The orbits of stellar binaries hosting planetary systems are typically wider than 100 AU and often highly inclined with respect to the planetary orbits. The effect of secular perturbations from such an inclined binary orbit on a coupled system of planets, however, is little understood theoretically. In this paper we investigate various dynamical classes of double-planet systems in binaries through numerical integrations and we provide an analytic framework based on secular perturbation theories. Differential nodal precession of the planets is the key property that separates two distinct dynamical classes of multiple planets in binaries: (1) dynamically-rigid systems in which the orbital planes of planets precess in concert as if they were embedded in a rigid disk, and (2) weakly-coupled systems in which the mutual inclination angle between initially coplanar planets grows to large values on secular timescales. In the latter case, the quadrupole perturbation from the outer planet induces additional Kozai cycles and causes the orbital eccentricity of the inner planet to oscillate with large amplitudes. The cyclic angular momentum transfer from a stellar companion propagating inward through planets can significantly alter the orbital properties of the inner planet on shorter timescales. This perturbation propagation mechanism may offer important constraints on the presence of additional planets in known single-planet systems in binaries.

*Subject headings:* celestial mechanics – binaries: general – planetary systems

### 1. INTRODUCTION

As of February 2008, among the 220 planet-hosting stars (excluding pulsars) 44 (20%) of them are members of binary or higher-order multiple-star systems (Raghavan et al. 2006; Desidera & Barbieri 2007; Eggenberger et al. 2007). Since the systematic adaptive-optics searches for stellar companions around known planetary systems are not yet complete, the true multiplicity among planet-hosting stars should be greater than 20% (Eggenberger et al. 2007). Many of the stellar companions around planetary systems are faint, distant, or both. Nearly a dozen of them are K-type or later (including eight M dwarf companions and one brown dwarf companion). Their sky-projected separations range from 20 to 12000 AU from the planetary systems, with a median of  $\sim 510$  AU. This occurrence of planets in relatively wide binaries is certainly affected by the observational biases. Spectroscopic binaries with angular separations 2–6'' are often deliberately excluded from the planet-search target samples since it is difficult to extract precise radial-velocity information from the recorded flux contributed from the two components (Valenti & Fischer 2005; Eggenberger et al. 2007). On the other hand, it is also shown by theoretical planet formation simulations that nearby stellar companions may hinder planet formation processes in multiple ways. First, a binary companion at a distance  $\sim 20$ –100 AU tends to tidally truncate the nascent circumstellar disk around the primary, thereby reducing the mass and lifetime of the disk (Artymowicz & Lubow 1994; Pichardo et al. 2005; Kley & Nelson 2007). Periodic tidal heating in the disk

caused by a companion would also lead to the decay of spiral structures and evaporation of the volatile materials (Nelson 2000; Mayer et al. 2005). Even if planetesimals successfully form in the disk, a close stellar companion would stir up their relative velocities so that they are likely to fragment through collisions rather than to coagulate (Kley & Nelson 2007). From most of these studies it is inferred that the orbital separations of stellar binaries containing planetary systems can be preferentially larger than the binary systems without planets.

Distant (and often faint) stellar companions, however, may still significantly alter the planetary orbits around the primary stars on secular timescales. Zucker & Mazeh (2002) were the first to investigate the statistical differences in the orbital properties of planets in binaries possibly caused by such secular perturbations. The most distinctive trend they found was the occurrence of massive close-in planets exclusively among binaries. Though they had only 9 planets in binaries in their samples at that time, this trend has been robust for planets with  $m \sin i > 2M_J$  and  $P < 100$  days as the sample size increased (see Udry & Santos 2007, and references therein). There are also discernible differences in the eccentricity–period diagram for different populations of extrasolar planets (Figure 1). It has been pointed out by Eggenberger et al. (2004) that planets in multiple-star systems show systematically lower orbital eccentricities if their orbital periods are less than 40 days. On the other hand, there is a relative paucity of planets in binaries on near-circular orbits ( $e < 0.1$ ), for planets with orbital periods greater than 40 days. Indeed, in this region the median orbital eccentricity of planets in binaries is 0.36, much higher than the median eccentricity 0.27 of planets around single stars. And lastly, the four largest orbital eccentricities and  $\sim 50\%$  of the 18 planets with  $e > 0.6$

<sup>1</sup> Department of Physics and Astronomy, Northwestern University, 2145 Sheridan Road, Evanston, IL 60208; g-takeda, r-kita, rasio@northwestern.edu

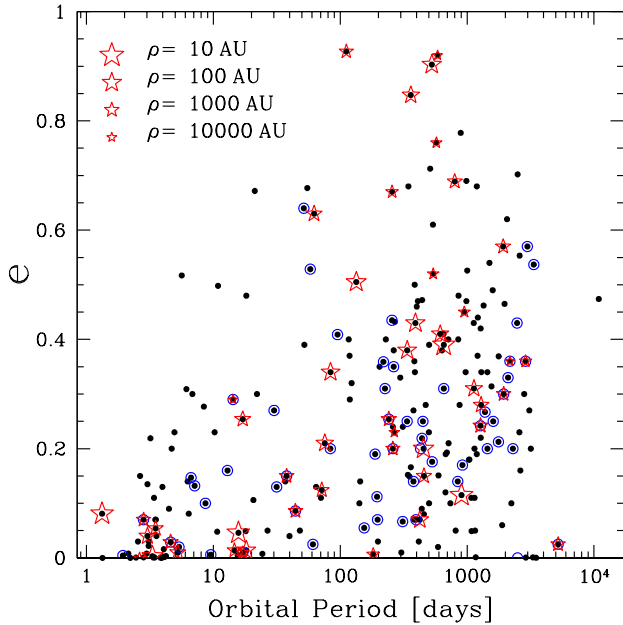


FIG. 1.— Eccentricity–period diagram for 234 extrasolar planets (black dots). The red-star symbols represent planets that are associated with binary companions, with the symbol sizes scaled to  $1/\log \rho$ , where  $\rho$  is the projected binary separation. The circled-dots are the members of multiple-planet systems.

are associated with confirmed binary companions. These statistical trends strongly suggest that the orbital evolution of planetary systems is commonly affected by distant stellar companions.

Theoretical studies have investigated the role of secular perturbations by stellar companions in the dynamical evolution of planetary systems using simplified models. The Kozai mechanism, originally discovered by Kozai (1962) for the orbital analysis of a Jovian asteroid under the perturbation from the Sun, has been adopted for extrasolar planets and successfully modeled some of the highly eccentric planetary orbits, assuming that those systems contain only one planet (Holman et al. 1997; Wu & Murray 2003). The Kozai mechanism permits the planet’s orbital eccentricity to stably grow to arbitrarily large values up to unity, by tuning the unknown mutual inclination between the planetary and binary orbits. Recently, there is growing attention on the combined effect of the Kozai mechanism and tidal dissipation mechanism as an alternative means to produce hot Jupiters (Wu & Murray 2003; Fabrycky & Tremaine 2007; Wu et al. 2007). For the cases of multiple-planet systems in binaries, Marzari et al. (2005) have systematically studied the dynamical outcomes of initially-packed triple-planet systems in binaries, for limited cases in which the planetary systems are coplanar with the binary.

The secular effect of a non-coplanar stellar companion to a coupled system of multiple planets is, however, an important problem which has received little attention in the past. In reality, planetary systems emerging from the nascent circumstellar disks are more likely to contain multiple planets (Ida & Lin 2005; Thommes et al. 2007). It is also rather unlikely that newly formed multiple planets orbit in the plane of the binary. Hale (1994) has sys-

tematically studied binary systems with solar-type components in search for the alignment of their spin axes, by combining the  $v \sin i$  measurements with rotational period information. His results showed that spin alignments exist only for relatively close binary systems with orbital separations 30–40 AU or less. Because the binary separations observed among planet-hosting stars are typically much beyond this limit, planetary systems formed along the primary’s equator are randomly inclined with respect to the binary plane. In other words, the distribution of the mutual inclination angle  $I$  between the planetary orbits and the binary plane is uniform in  $\cos I$ . This implies that for about three-quarter of the cases planetary orbits are inclined with respect to the binary plane by more than  $40^\circ$ , the critical Kozai angle (§ 2.1).

The effects of Kozai-type perturbations to multiple-planet systems were first investigated by Innanen et al. (1997). While numerically studying the evolution of the Solar System under the influence of a hypothetical stellar companion orbiting at 400 AU from the Sun, they discovered that, under certain circumstances, the orbital elements of the giant planets evolve in concert, as if they were embedded in a rigid disk. Malmberg et al. (2007) have performed similar numerical experiments but with slightly different binary parameters. In their simulations, the orbital evolutions of the planets were decoupled, and the excited orbital eccentricities of the planets induced instability and led to ejection of one or more planets.

The rigid coupling between planets in response to the binary perturbation found by Innanen et al. (1997) has not been understood analytically. A significant challenge is involved in developing a generalized perturbation theory for  $N$ -body systems with  $N > 3$  since the approximation techniques employed in the traditional secular theories are no longer valid. Higher order terms in the orbital eccentricities, inclinations, and semi-major axes may play important roles in the long-term evolution of multiple planets in binaries and thus cannot be eliminated from the disturbing function as in typical secular theories. Systematic mapping of dynamical stabilities using numerical integrations is also impractical due to the large number of dimensions of the parameter space (the mass and the three-dimensional orbits for each planet and the binary).

The objective of this paper is to investigate the secular evolution of two planets in wide binaries with a more generalized set of initial conditions and to provide analytic criteria that separate possible dynamical outcomes. To disentangle the complex interplay between binary perturbations and gravitational coupling between planets, we first separate the problem into two sets of secular three-body problems: the secular evolution of hierarchical, highly inclined triple systems (the Kozai mechanism, § 2.1) and the secular evolution of isolated, near-coplanar double-planet systems (the Laplace-Lagrange secular theory, § 2.2). In § 3, we list the important dynamical classes of double-planet systems in binaries along with numerical simulations. The analytic explanation for each of the dynamical classes is presented in § 4.

## 2. SECULAR THREE-BODY PROBLEMS

In this paper we focus on hierarchical four-body systems in which two planets orbit a component of a wide stellar binary system. The binary separation is typically

on the order of 100 AU. The initial planetary orbits are assumed to be nearly coplanar and arbitrarily inclined with respect to the binary plane.

To analyze the long-term evolution of hierarchical four-body systems, we first consider the gravitational perturbation from the stellar companion and the mutual perturbations between the planets separately. The former has been studied in detail in the context of the Kozai mechanism, which takes account of full three dimensional orbits, assuming the hierarchy of the system. The latter is the secular evolution of a pair of planets around a single star, analytically formulated through the Laplace-Lagrange theory, which does not assume any hierarchy but uses the assumption of small orbital inclinations and eccentricities. Both theories are developed by collecting only the secularly varying terms from the time-averaged disturbing function. This is an important point, indicating that these secular perturbations are generally not cumulative; a secular perturbation mechanism occurring on a longer timescale is averaged out to zero by the other perturbation (there are rare cases of secular resonances between two different perturbation mechanisms, discussed in § 3.3). In the following sections we summarize the relevant properties of Kozai-type perturbations and the Laplace-Lagrange secular theory, and derive the secular perturbation timescales of each mechanism.

Throughout this paper, subscripts 0, 1, 2, and B are used to refer to the properties of the primary star, the inner planet, the outer planet, and the binary companion, respectively.

### 2.1. The Kozai Mechanism

The secular perturbation theory for a hierarchical, non-coplanar triple system was first developed by Kozai (1962) in the analysis of the motion of a Jovian asteroid under the gravitational attraction of the Sun. Here we adopt the Kozai mechanism for the orbital evolution of a planet around a component of a wide binary system.

The complete Hamiltonian of the three-body system is

$$\mathcal{F} = -\frac{Gm_0m_1}{2a_1} - \frac{G(m_0+m_1)m_B}{2a_B} + \mathcal{F}'. \quad (1)$$

The formulation of the Kozai mechanism takes advantage of the hierarchy of the system such that  $\alpha \equiv a_1/a_B \ll 1$  and expands the perturbing Hamiltonian  $\mathcal{F}'$  in terms of  $\alpha$  as

$$\mathcal{F}' = -\frac{G}{a_B} \sum_{j=2}^{\infty} \alpha^j M_j \left(\frac{r_1}{a_1}\right)^j \left(\frac{a_B}{r_B}\right)^{j+1} P_j(\cos \Phi), \quad (2)$$

where  $\alpha \equiv a_1/a_B$ ,  $\mathbf{r}_1$  is the vector from  $m_0$  to  $m_1$ ,  $\mathbf{r}_B$  is the vector from the barycenter of  $m_0$  and  $m_1$  to  $m_B$ ,  $\Phi$  is the angle between  $\mathbf{r}_1$  and  $\mathbf{r}_B$ ,  $P_j(\cos \Phi)$  is the Legendre polynomial, and

$$M_k = m_0m_1m_B \frac{m_0^{j-1} - (-m_1)^{j-1}}{(m_0+m_1)^j} \quad (3)$$

(Harrington 1968; Lee & Peale 2003). Since  $\alpha$  is small,  $\mathcal{F}'$  is a rapidly converging series. The first term of  $\mathcal{F}'$  is the quadrupole-order potential ( $j=2$ ) explicitly written as

$$\mathcal{F}_q = -\frac{Gm_0m_1m_B}{m_0+m_B} \frac{r_1^2}{r_B^3} P_2(\cos \Phi) \quad (4)$$

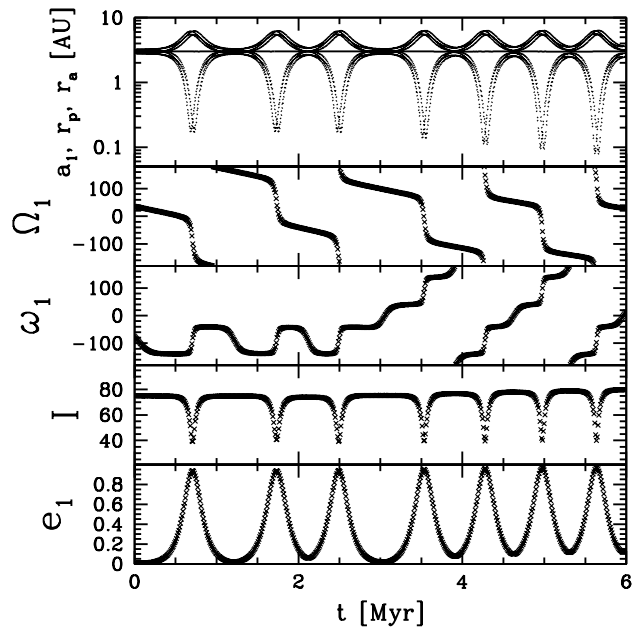


FIG. 2.— Numerically simulated orbital evolution of a planet in a binary with an initial inclination angle  $I = 75^\circ$ . The orbital elements are, from the bottom, eccentricity ( $e$ ), inclination ( $I$ ), argument of pericenter ( $\omega$ ), longitude of ascending node ( $\Omega$ ), and semi-major axis ( $a$ ), pericenter ( $r_p$ ) and apocenter ( $r_a$ ) distances. All the angles are shown in degrees. Each cross is separated by  $10^4$  yr. The orbital elements evolve on similar timescales during the Kozai cycles, while the semi-major axis remains constant.

(Ford et al. 2000), where the second-degree Legendre Polynomial is  $P_2(\cos \Phi) = (3 \cos^2 \Phi - 1)/2$ . To derive the secular equations of motion, short-period terms such as  $\Phi$  are eliminated through averaging the Hamiltonian over the mean anomalies,  $l_1$  and  $l_B$ . The averaged quadrupolar Hamiltonian is (Fabrycky & Tremaine 2007),

$$\bar{\mathcal{F}}_q = -\frac{Gm_0m_1m_B}{m_0+m_1} \frac{a_1^2}{8a_B^3(1-e_B^2)^{3/2}} \times [2 + 3e_1^2 - (3 + 12e_1^2 - 15e_1^2 \cos^2 \omega_1) \sin^2 I]. \quad (5)$$

Since the binary orbit carries the majority of the angular momentum of the system, it is typically taken as the reference plane ( $I_B = 0^\circ$ ) that is invariant in the quadrupole approximation. Thus the angle  $I$  in Equation 6 corresponds to the relative inclination of the planetary orbit measured from the reference plane. With the averaged Hamiltonian, the Lagrange equations of motion can be derived (Equations 5 of Innanen et al. 1997) which can be numerically integrated for  $e_1(t)$ ,  $I_1(t)$ ,  $\omega_1(t)$ , and  $\Omega_1(t)$  (Figure 2).

Now we list the key properties of the Kozai Mechanism.

(1) The canonical Delaunay elements of the planet are the mean anomaly  $l_1$ , the argument of pericenter,  $\omega_1$  and the longitude of ascending node  $\Omega_1$ , associated with their canonical conjugates  $L_1 = m_0m_1\sqrt{Ga_1/(m_0+m_1)}$ ,  $G_1 = L_1\sqrt{1-e_1^2}$ , and  $H_1 = G_1 \cos I$ , respectively (Harrington 1968). Since the mean anomaly  $l_1$  is deliberately removed from the averaged Hamiltonian, its canonical conjugate momentum  $L_1 \equiv m_0m_1\sqrt{Ga_1/(m_0+m_1)}$  and thus also the semi-major axis are constants of motion. Because the averaged Hamiltonian is independent of  $\Omega_1$ , its canonical conjugate  $H_1$ , corresponding to the

z-component angular momentum, is also constant. This implies that the averaged Hamiltonian is axisymmetric. Another integral of motion, called the Kozai integral, can be defined as

$$\frac{H}{L} = \sqrt{1 - e_1^2} \cos I \equiv \sqrt{h}. \quad (7)$$

The Kozai integral couples the evolution of the eccentricity and the inclination during Kozai cycles.

(2) When the mutual inclination between the two orbits is small, the argument of pericenter of a planet secularly circulates in the quadrupolar potential of the binary. However, Kozai (1962) discovered that if the inner planetary orbit is sufficiently inclined with respect to the binary orbit such that  $h < 0.6$ , there is a libration solution possible for the planetary orbit; the planet’s pericenter argument secularly oscillates around either one of the two fixed points,  $\pm 90^\circ$ . If the octupole term is included in the perturbing Hamiltonian, the pericenter argument in fact is permitted to alternate between circulation and libration (Ford et al. 2000), as illustrated in Figure 2. The critical Kozai angle corresponding to  $h = 0.6$  is  $I_{\text{koz}} = 39.23^\circ$  for a planet with initially small orbital eccentricity.

(3) If the initial mutual inclination  $I_0$  is above the critical Kozai angle (including a retrograde planetary orbit) such that  $I_0 \in [I_{\text{koz}}, 180^\circ - I_{\text{koz}}]$ , then the orbital eccentricity of the planet secularly oscillates with a large amplitude (Figure 2). The evolution of the orbital inclination is coupled to the eccentricity oscillation through the Kozai integral, and  $I$  oscillates between  $I_{\text{koz}}$  and  $I_0$ .

(4) The averaged quadrupolar Hamiltonian  $\mathcal{F}_q$  is conserved since it is independent of time. Because the semi-major axis is also constant, a conserved quantity can be defined from the Equation (6),

$$C \equiv 2 + 3e_1^2 - (3 + 12e_1^2 - 15e_1^2 \cos^2 \omega_1) \sin^2 I = \text{constant}. \quad (8)$$

This implies that the maximum orbital eccentricity of the planet  $e_{1,\text{max}}$  occurs when  $\omega_1 = \pm 90^\circ$ . Thus,  $e_{1,\text{max}}$  can be written as a function of  $C$  and  $h$ , which are determined from the initial condition. If we assume that the planetary orbit is initially nearly circular so that  $e_{1,0} \ll 1$ , then  $C$  and  $h$  are dependent only on the initial mutual inclination  $I_0$ , and the maximum orbital eccentricity can be predicted by a simple formula

$$e_{1,\text{max}} \approx \sqrt{1 - \frac{5}{3} \cos^2 I_0}. \quad (9)$$

This approximation is sufficiently accurate in the limit  $e_{1,0} \lesssim 0.2$  (Fabrycky & Tremaine 2007).

(5) The longitude of ascending node of the planet secularly circulates, completing one cycle while the orbital inclination and the eccentricity oscillate roughly twice (Figure 2). This is because of the mirror symmetry of the planetary orbit with respect to the  $I = 90^\circ$  plane. The rotation of the planet’s nodal line in the binary plane is equivalent to and better visualized as the precession of the orbital angular momentum vector  $\mathbf{L}_1$  around the normal of the reference plane (= the orbital angular momentum vector of the binary,  $\mathbf{L}_B$ ). Figure 3 illustrates the nodal precession of a planetary orbit in a binary. The angle  $I$  between the two vectors  $\mathbf{L}_1$  and  $\mathbf{L}_B$  corresponds to the mutual inclination between the orbits.

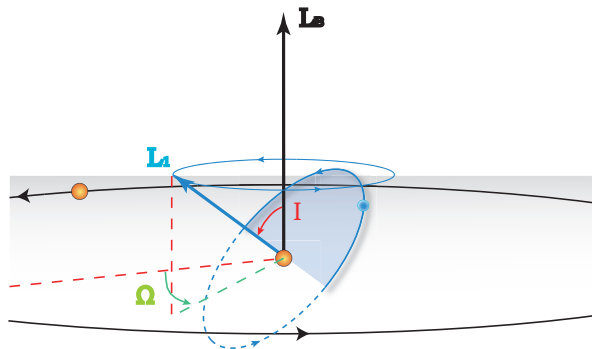


FIG. 3.— Nodal precession of a planet forced by a binary perturbation. As the nodal line of the planetary orbit rotates in the orbital plane of the binary, the angular momentum vector of the planet  $\mathbf{L}_1$  sweeps a cone shape around the angular momentum vector of the binary  $\mathbf{L}_B$ . If the initial inclination  $I_0$  is above the critical Kozai angle  $I_{\text{koz}}$ , the mutual inclination  $I$  also oscillates roughly twice between  $I_0$  and  $I_{\text{koz}}$  during one nodal circulation cycle.

The nodal precession of a planet in the Kozai solution is always monotonic circulation unlike the pericenter precession, which may alternate between libration and circulation. This is because  $\Omega_1$  is measured only from an arbitrary reference direction whereas for  $\omega_1$  there exists a fixed line of reference which is the nodal line of the planetary orbit in the binary plane. Thus, the circulation of the planetary ascending node naturally results from secular three-body interaction and it does not require any critical angle.

(6) The characteristic timescale of the Kozai mechanism can be estimated as (Kiseleva et al. 1998)

$$\tau_{\text{Koz}} \approx \frac{2}{3\pi} \frac{P_B^2}{P_1} (1 - e_B^2)^{3/2} \frac{m_0 + m_1 + m_B}{m_B}. \quad (10)$$

As seen in Figure 2, the orbital elements  $e_1$ ,  $I_1$ ,  $\omega_1$ , and  $\Omega_1$  all evolve roughly on this timescale. This is why it is often called the “Kozai resonance”, although it is not strictly a resonant interaction (Kinoshita & Nakai 1999).

(7) When there is another source of secular perturbation for the planetary orbit on a timescale shorter than  $\tau_{\text{Koz}}$ , this can suppress the Kozai cycles. Competing perturbations include general relativistic (GR) precession, tidal and rotational bulges of the host star, and other planets in the system (Wu & Murray 2003; Fabrycky & Tremaine 2007). If any one of these perturbations causes the pericenter of a planet to precess faster than does the Kozai mechanism, then the weak secular torque from the binary companion secularly averages to zero, and the Kozai cycles become completely suppressed.

## 2.2. Secular Gravitational Coupling Between Planets

The secular evolution of a pair of planets through mutual gravitational perturbations has been well-formulated in the second-order Laplace-Lagrange secular theory (“L-L theory”, hereafter). The L-L theory also employs orbital averaging and elimination of short-period terms to isolate the secular terms in the disturbing potential. However, the L-L theory does not assume any hierarchy in the planetary system as does the Kozai theory. The L-L theory is valid for any value of  $\alpha \equiv a_1/a_2$  as long as the orbital separation between the planets is sufficiently large so that there is no short-term perturbation.

In the L-L theory the simplified disturbing function for each planet is derived by eliminating the terms that are dependent on the mean longitudes (which vary on short timescales) and also the terms that are dependent only on the semi-major axes (which remain constant). Up to the second order in the eccentricities and the inclinations, the eccentricity and inclination perturbations are decoupled and thus the disturbing functions can be written separately (in the fourth-order terms the evolutions of  $e$  and  $I$  become coupled when they are large; see Veras & Armitage 2007).

The second-order secular disturbing functions for the inner and the outer planets in the  $e-\varpi$  space are (Brouwer & Clemence 1961; Murray & Dermott 1999)

$$\mathcal{R}_1^{(e,\varpi)} = n_1 a_1^2 \left[ \frac{1}{2} A_{11} e_1^2 + A_{12} e_1 e_2 \cos(\varpi_1 - \varpi_2) \right], \quad (11)$$

$$\mathcal{R}_2^{(e,\varpi)} = n_2 a_2^2 \left[ \frac{1}{2} A_{22} e_2^2 + A_{21} e_1 e_2 \cos(\varpi_1 - \varpi_2) \right], \quad (12)$$

where  $n$  is the mean motion and  $\varpi$  is the longitude of pericenter, and  $A_{ij}$  are the matrix elements determined by the masses and semi-major axes. The eigenvalues  $g_+$  and  $g_-$  of the matrix  $A$  correspond to the eigenfrequencies of the system and can be computed from the initial conditions (Zhou & Sun 2003),

$$g_+ = \frac{1}{2} \left[ (\Lambda_1 + \Lambda_2) + \sqrt{(\Lambda_1 - \Lambda_2)^2 + 4\Lambda_0^2 \Lambda_1 \Lambda_2} \right], \quad (13)$$

$$g_- = \frac{1}{2} \left[ (\Lambda_1 - \Lambda_2) + \sqrt{(\Lambda_1 - \Lambda_2)^2 + 4\Lambda_0^2 \Lambda_1 \Lambda_2} \right]. \quad (14)$$

The constants are determined as

$$\Lambda_0 = -\frac{A_{12}}{A_{11}} = -\frac{A_{21}}{A_{22}} \approx \frac{5}{4} \alpha \left( 1 - \frac{1}{8} \alpha^2 \right), \quad (15)$$

$$\Lambda_1 = A_{11} = \frac{1}{4} n_1 \frac{m_2}{m_0 + m_1} \alpha^2 b_{3/2}^{(1)}(\alpha), \quad (16)$$

$$\Lambda_2 = A_{22} = \frac{1}{4} n_2 \frac{m_1}{m_0 + m_2} \alpha b_{3/2}^{(1)}(\alpha), \quad (17)$$

where the Laplace coefficient  $b_{3/2}^{(1)}(\alpha)$  is defined as

$$b_{3/2}^{(1)}(\alpha) = \frac{1}{\pi} \int_0^{2\pi} \frac{\cos \psi d\psi}{(1 - 2\alpha \cos \psi + \alpha^2)^{3/2}}. \quad (18)$$

The approximation for  $\Lambda_0$  is accurate (less than 5% error) for systems with  $\alpha \lesssim 0.9$  (Zhou & Sun 2003).

The eigenvalues  $g_+$  and  $g_-$  are the characteristic frequencies at which the orbital elements evolve. For example, in the secular solutions orbital eccentricities of the planets oscillate with a period  $\tau = 2\pi/|g_+ - g_-|$ . The solution for the longitudes of pericenter is more complex as it is a non-linear combination of the two eigenmodes. However, it can be easily shown from the L-L solutions that in the following limit

$$\xi \equiv \frac{\alpha}{1 - 3q\sqrt{\alpha}/b_{3/2}^{(1)}} \ll 1 \quad (19)$$

where  $q = m_2/m_1$ , then the  $g_-$ -mode corresponds to the simple pericenter precession of the more massive planet, and  $g_+$ -mode corresponds to the pericenter precession of the less massive planet. Because we are mainly interested in hierarchical planetary systems in which the

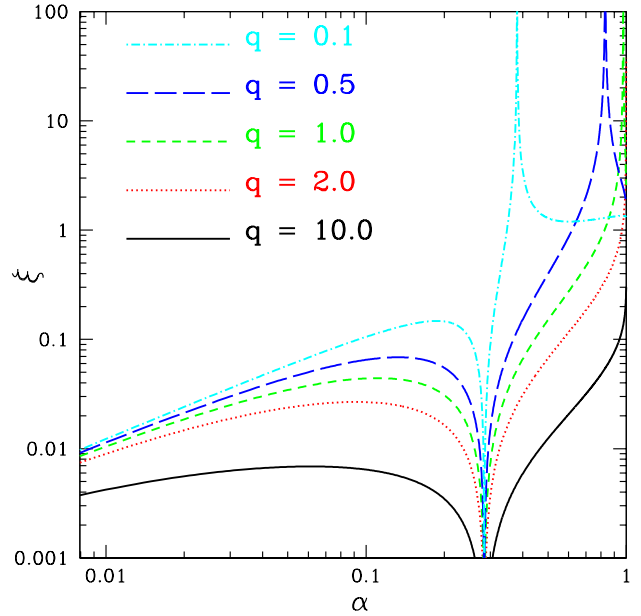


FIG. 4.— The parameter  $\xi$  described in Eq. (19) as a function of the semi-major axis ratio  $\alpha$  for different mass ratios  $q \equiv m_2/m_1$ . If  $\xi \ll 1$ , the eigenfrequencies  $g_+$  and  $g_-$  derived from the L-L theory correspond to the pericenter precession frequencies of the planets. For all the systems discussed in § 3,  $\xi \ll 0.1$ .

secular perturbation from the stellar companion to  $m_2$  dominates over the perturbation from  $m_1$  to  $m_2$ , it turns out that  $\xi$  is at most 0.1 or typically much smaller for all the systems discussed in § 3. Thus, we will use the derived eigenfrequencies to provide estimates for the pericenter precession timescales  $\tau_{pp,1}$  and  $\tau_{pp,2}$  for the inner and outer planets, respectively, as

$$\left. \begin{aligned} \tau_{pp,i} &= 2\pi/g_+ \\ \tau_{pp,j} &= 2\pi/g_- \end{aligned} \right\} \text{ with } m_i < m_j \text{ (} i, j = 1, 2; i \neq j \text{)}. \quad (20)$$

Next, the disturbing functions in the  $I-\Omega$  space are

$$\mathcal{R}_1^{(I,\Omega)} = n_1 a_1^2 \left[ \frac{1}{2} B_{11} I_1^2 + B_{12} I_1 I_2 \cos(\Omega_1 - \Omega_2) \right], \quad (21)$$

$$\mathcal{R}_2^{(I,\Omega)} = n_2 a_2^2 \left[ \frac{1}{2} B_{22} I_2^2 + B_{21} I_1 I_2 \cos(\Omega_1 - \Omega_2) \right], \quad (22)$$

where the matrix  $B$  is similar to  $A$ , with slight differences in the signs and the Laplace coefficients. The eigenvalues of the matrix  $B$  are

$$f_1 = 0, \quad (23)$$

$$f_2 = \Lambda_1 + \Lambda_2. \quad (24)$$

Note that there is a subtle difference compared to the solution in the  $e-\varpi$  space that two planets around a spherical star have only one secular frequency in the  $I-\Omega$  space. This is because the orbital inclination is a relative quantity that requires an arbitrary reference plane, whereas the orbital eccentricity is a well-defined quantity and introduces asymmetry in the coordinate system. There is in fact only one physically meaningful inclination angle for two planets, which is their mutual inclination. If, however, the oblateness of the star is introduced, it would break the degeneracy of the problem, and the L-L theory

would yield two eigenfrequencies in the  $I$ - $\Omega$  space. We neglect the quadrupolar perturbation from the central star and thus derive the single nodal precession timescale  $\tau_{\Omega\text{pp}}$  of the planets as

$$\tau_{\Omega\text{pp}} = 2\pi/f_2. \quad (25)$$

### 2.3. Apsidal and Nodal Coupling of Planets

A pair of planets around a single star can undergo either independent pericenter precessions (apsidal circulation) or coupled pericenter precessions (apsidal libration). If the planets follow apsidal libration, then  $\Delta\varpi(t) \equiv |\varpi_1(t) - \varpi_2(t)| < C_{\text{amp}} + C_{\text{fixed}}$  at any given time  $t$ , where  $C_{\text{amp}} < \pi/2$  is the libration amplitude. There are two different modes of apsidal libration:  $C_{\text{fixed}} = 0$  corresponds to the aligned libration, and  $C_{\text{fixed}} = \pi$  corresponds to the anti-aligned libration. Using the secular solutions of the L-L theory, Zhou & Sun (2003) have provided the explicit analytical criteria for the occurrence of apsidal librations given the initial orbital parameters as

$$\frac{e_2}{e_1} \Big|_{\text{initial}} < -\frac{5\mu\alpha^{3/2}(1-\alpha^2/8)}{2(1-\mu\alpha^{1/2})} \cos \Delta\varpi_0, \quad (26)$$

or,

$$\frac{e_2}{e_1} \Big|_{\text{initial}} > \frac{2}{5} \frac{1-\mu\alpha^{1/2}}{\alpha(1-\alpha^2/8)} \frac{1}{\cos \Delta\varpi_0} > 0, \quad (27)$$

where  $\mu \equiv m_1/m_2$  and  $\Delta\varpi_0 \equiv |\varpi_1 - \varpi_2|_{\text{initial}}$ . Zhou & Sun (2003) called the libration regions defined by Equations (26) and (27) down- and up-librations, respectively.

For two planets orbiting around a single star, whether the system secularly undergoes apsidal libration or circulation can be determined from the initial orbital configurations. With the perturbation from a stellar companion, however, the above criteria need to be evaluated for each snapshot of time, and the planets may alternate between libration and circulation.

The role of various external perturbations in affecting the secular apsidal precession mode of planets have been previously investigated by several authors (e.g., Malhotra 2002; Chiang & Murray 2002; Ford et al. 2005). Chiang & Murray (2002) have analyzed the secular evolution of the outer two planets c and d of the  $\nu$  Andromedae system and discovered that an adiabatic eccentricity excitation to the outermost planet d caused by a remnant gaseous disk exterior to the planets would naturally bring the planets c and d into small-amplitude apsidal libration. In this dynamical scenario, there are two effects caused by the outer gas disk to the orbit of the outer planet: the secular precession of  $\varpi_d$  (and thus change in  $\cos \Delta\varpi_0$ ), and the adiabatic growth of the eccentricity ratio  $e_d/e_c$ . Since  $1-\mu\alpha^{1/2} > 0$  for  $\nu$  And c and d, these two effects bring the system into the aligned up-libration as defined in Eq. (27). Once this up-libration criterion is met, the two planets remain on libration trajectories, maintaining  $\Delta\varpi < \pi/2$ . As the eccentricity growth of the outer planet continues, the libration amplitude further damps down toward  $\Delta\varpi = 0$ .

Similar apsidal capture mechanism may follow when the outer planet of a double-planet system is perturbed by a binary companion through the Kozai mechanism.

Because the condition that the Kozai cycles on the outer planet not be suppressed favors orbital configurations such that  $1 - \mu\alpha^{1/2} > 0$ , the most common result from a binary perturbation is the capture into aligned up-libration (Eq. (27)). We present specific examples of different apsidal precession modes as well as their effects on the eccentricity evolution of planets in binaries in more detail in § 3.3.

The ascending nodes of a pair of planets can also secularly circulate or librate. The analytical nodal libration criteria are (Zhou & Sun 2004)

$$\frac{I_2}{I_1} \Big|_{\text{initial}} < \frac{2\mu\alpha^{1/2}}{\mu\alpha^{1/2} - 1} \cos \Delta\Omega_0, \quad (28)$$

or,

$$\frac{I_2}{I_1} \Big|_{\text{initial}} > \frac{1}{2}(1 - \mu\alpha^{1/2}) \frac{1}{\cos \Delta\Omega_0} \quad (29)$$

where  $\Delta\Omega_0 \equiv |\Omega_1 - \Omega_2|_{\text{initial}}$ . As previously mentioned, without the presence of external perturbations, the ascending nodes of two planets precess at one characteristic frequency. If another source of nodal perturbation, for example a secular perturbation from a stellar companion, introduces additional nodal precession to one of the planets, then the nodal offset  $\Delta\Omega$  of the planets may also secularly circulate or librate.

Figure 5 illustrates the motion of the orbital angular momentum vectors for nodally circulating and librating systems. In a system in which the nodal coupling between the planets is weak compared to an external perturbation, the orbital angular momentum vectors  $\mathbf{L}_1$  and  $\mathbf{L}_2$  independently precess around the normal of the reference plane ( $= \mathbf{L}_B$  for the case of planets in a binary). Notice that in a nodally circulating system, the mutual inclination angle  $I_{12}$  between the two planetary orbits determined as

$$\cos I_{12} = \cos I_1 \cos I_2 + \sin I_1 \sin I_2 \cos(\Omega_1 - \Omega_2) \quad (30)$$

oscillates within a large range, and the planetary orbits no longer remain coplanar. In a nodally librating planetary systems, the maximum mutual inclination angle is limited by the nodal libration amplitude. In Figure 5 (b),  $\mathbf{L}_2$  secularly circulates around  $\mathbf{L}_B$  due to the perturbation from the binary while  $\mathbf{L}_1$  precesses around  $\mathbf{L}_2$  maintaining a small angle between the two vectors. If the nodal coupling between the planets is sufficiently strong and thus the nodal libration amplitude remains small, the planetary orbits can remain nearly coplanar as they secularly evolve. The rate of nodal precession  $\sim 1/\tau_{\Omega\text{pp}}$  determined from Eq. (25) is an important measure to scale the nodal-coupling strength of planets. If an external perturber precesses the ascending node of one of the planets at a greater rate, large-amplitude nodal libration or nodal circulation will follow, and the planets will open a large mutual inclination angle between their orbits.

### 3. DYNAMICAL CLASSES OF DOUBLE-PLANET SYSTEMS IN BINARIES

We find that there are three distinct dynamical classes of double-planet systems in binaries: (i) completely decoupled systems in which planetary orbits are independently affected by the binary perturbation; (ii) weakly coupled systems in which a large mutual inclination angle grows between the planetary orbits due to large-

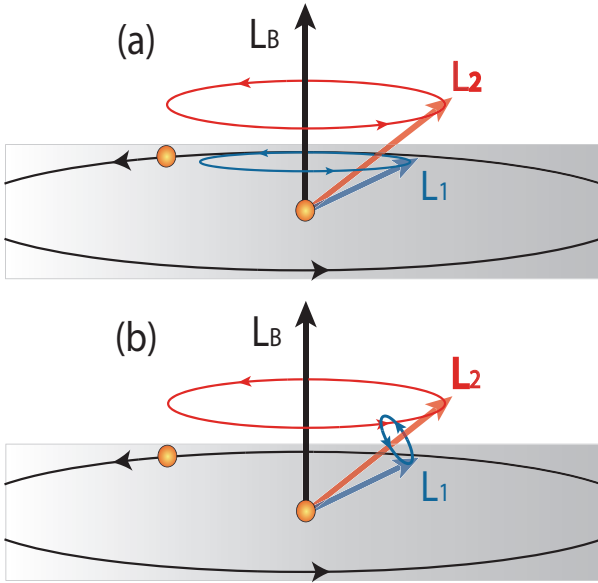


FIG. 5.— The precession of the orbital angular momentum vectors of double-planet systems in binaries that are (a) in nodal circulation and (b) in nodal libration.

amplitude nodal libration; (iii) strongly coupled, dynamically rigid systems in which the inclinations and the ascending nodes of the planets evolve in concert.

Each dynamical class is presented with a numerical simulation. For all the numerical simulations, we have used the integration package MERCURY 6.2 (Chambers 1999) with the Bulirsch-Stoer mode to accurately account for possible occurrence of close encounters between planets. The general relativistic accelerations are also included in the integrations to treat the additional orbital precession of planets when they are sufficiently close to the primary star. The initial planetary orbits are selected to be nearly coplanar ( $I_{12} < 5^\circ$ ) and circular ( $e < 0.1$ ), and the Hill stability criterion (Gladman 1993) is checked to ensure no immediate planet-planet scattering. Each simulation is run for at least five Kozai timescales of the outer planet ( $\sim 5P_B^2/P_2$ ).

### 3.1. Evolution of Decoupled Planets in Binaries

Figure 6 illustrates the orbital evolution of a pair of dynamically decoupled planets in a binary following independent Kozai cycles. The planetary system is largely hierarchical, consisting of an inner Jupiter-mass planet at 2 AU and an outer  $\sim 10M_\oplus$  planet at 32 AU. Due to the large orbital separation between the planets and the small mass of the outer planet, the mutual gravitational interaction of the planets is completely suppressed by the perturbation from the stellar companion. This system can be viewed as two non-interacting test particles placed in a quadrupole potential of a binary, resulting in independent Kozai cycles. Since both planets are initially inclined by  $50^\circ$  with respect to the binary plane, their orbital eccentricities oscillate with roughly equal amplitudes. The orbital inclinations of the planets  $I_1$  and  $I_2$  measured from the binary plane also oscillate with the same amplitudes, between the initial value of  $50^\circ$  and the critical Kozai angle  $I_{\text{koz}} \sim 40^\circ$ .

Notice, however, that the initial coplanarity between

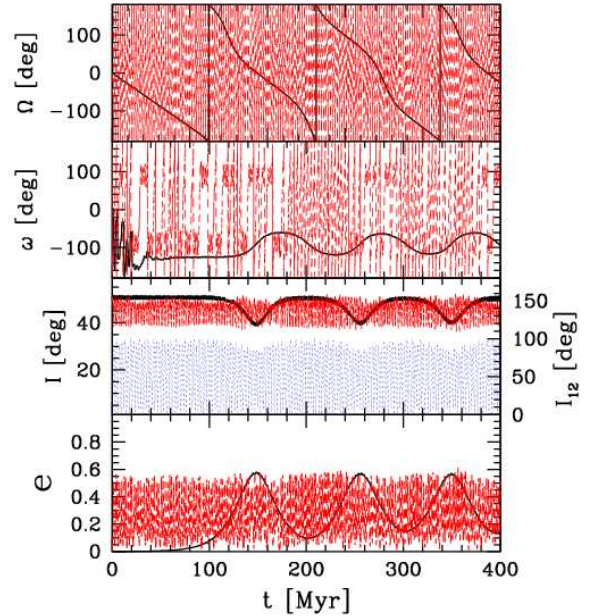


FIG. 6.— A pair of gravitationally decoupled planets undergoing independent Kozai cycles. The initial orbital parameters of the system are: for the inner planet (slowly varying black curve),  $m_1 = 1.0M_J$ ,  $a_1 = 2.0$  AU,  $e_1 = 0.01$  and  $I_1 = 50^\circ$ ; for the outer planet (rapidly moving red curve),  $m_2 = 0.032M_J$ ,  $a_2 = 31.6$  AU,  $e_2 = 0.01$  and  $I_2 = 50^\circ$ ; and for the binary companion,  $M_B = 1.0M_\odot$ ,  $a_B = 750$  AU and  $e_B = 0.20$ . The two ascending nodes are precessing independently. Consequently, the mutual inclination  $I_{12}$  (dotted blue curve, scale shown on the right axis) between the planetary orbits oscillates on the Kozai timescale of the outer planet ( $\tau_{\text{koz},2} \sim 2$  Myr) between  $0^\circ$  and  $\sim 100^\circ$ .

the planetary orbits is not maintained at all throughout the evolution. Due to the secular perturbation from the stellar companion, the orbital angular momentum vector  $\mathbf{L}_2$  of the outer planet precesses on a timescale  $\sim 2\tau_{\text{koz},2} \approx 2$  Myr, while the orbital angular momentum vector  $\mathbf{L}_1$  of the inner planet precesses similarly but on a much larger timescale  $\sim 2\tau_{\text{koz},1} \approx 200$  Myr (see also Figure 5 (a)). Thus the nodal difference  $\Delta\Omega$  between the planets secularly circulates on the timescale  $\tau_{\text{koz},2}$ , causing the mutual inclination  $I_{12}$  (which is a function of  $\Delta\Omega$ , see Eq. 30) to also oscillate on the same timescale with large amplitudes. The planetary orbits are maximally inclined with respect to each other every time their nodes are anti-aligned, reaching  $I_{12,\text{max}} \approx 100^\circ$ , nearly twice their initial inclinations with respect to the binary orbit.

In this example the two planets are dynamically invisible to each other since their secular mutual interaction is completely suppressed by the perturbation from the stellar companion. Thus, even though the mutual inclination  $I_{12}$  between their orbits grows beyond the critical Kozai angle  $I_{\text{koz}}$  for a large fraction of time, there is no additional perturbation induced to either planet.

### 3.2. Weakly Coupled Planets and Induced Eccentricity Oscillations

Next, we focus on more relevant systems in which (i) the evolution of the outer planet  $m_2$  is dominated by the secular perturbation from the stellar companion, and (ii) the evolution of the inner planet  $m_1$  is unaffected by the stellar companion but affected by the secular torque from

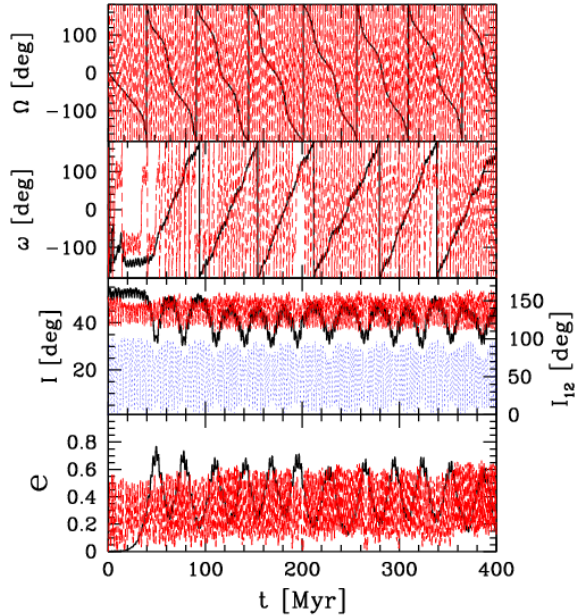


FIG. 7.— A weakly coupled, nodally circulating double-planet system in a binary. The system is identical to Fig. 6 except that the outer planet’s mass is increased to  $m_2 = 0.32M_J$ . Due to the increased perturbation by the outer planet, the eccentricity of the inner planet oscillates more rapidly compared to Fig. 6.

the outer planet.

The example in Figure 7 is integrated from the same initial conditions as those used in Figure 6, except for the outer planet’s mass increased by a factor of 10 so that  $m_2 = 0.32M_J$ . The increased perturbation from the outer planet now suppresses the binary perturbation on the inner planet’s orbit. The nodal precession periods are  $\sim 2$  Myr for the outer planet (due to the binary) and  $\sim 40$  Myr for the inner planet (due to the outer planet). Even though the evolution of the inner planet is now coupled to the outer planet, the planets are in nodal circulation, i.e., their orbital angular momentum vectors  $\mathbf{L}_1$  and  $\mathbf{L}_2$  precess independently, and the mutual inclination  $I_{12}$  oscillates between  $0^\circ$  and  $\sim 100^\circ$ , similarly to the previous example. The difference here, however, is that the Kozai cycles of the inner planet are introduced by the outer planet whose time-averaged inclination with respect to the inner planet is  $\sim 50^\circ$ . Notice that in this case the angular momentum transferred from the binary through the outer planet accelerates the eccentricity oscillation of the inner planet. The Kozai timescale of the inner planet is  $\sim P_2^2/(P_1 m_2) = 40$  Myr, shorter than  $\sim 100$  Myr in the previous example where the inner planet is directly perturbed by the stellar companion.

The secular dynamics of the planets changes drastically when the coupling strength between the planets is further increased. In Figure 8 the outer gas giant with a mass  $m_2 = 0.6M_J$  at  $a_2 = 12.7$  AU follows steady Kozai cycles, unaffected by the inner super-Earth with  $m_1 = 6.4M_\oplus$  at  $a_1 = 0.9$  AU. The binary perturbation to the inner planet is completely suppressed due to the much stronger secular torque applied by the outer planet’s orbit.

In this system, the two planets secularly follow large-amplitude nodal libration. As illustrated in Figure 5 (b), in this case the trajectory of the inner planet’s orbital

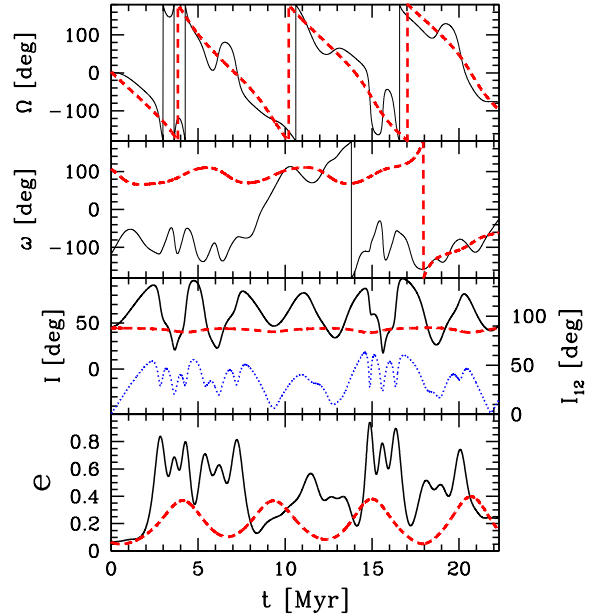


FIG. 8.— A weakly coupled, nodally librating double-planet system in a binary. The initial orbital parameters of the system are: for the inner planet (solid black curve),  $m_1 = 0.02M_J$ ,  $a_1 = 0.9$  AU,  $e_1 = 0.07$  and  $I_1 = 46^\circ$ , for the outer planet (dashed red curve),  $m_2 = 0.6M_J$ ,  $a_2 = 12.7$  AU,  $e_2 = 0.07$  and  $I_2 = 45^\circ$ , and for the binary companion,  $M_B = 0.7M_\odot$ ,  $a_B = 803$  AU and  $e_B = 0.78$ . The binary orbit is initially set at  $I_B = 0^\circ$ . The dotted blue curve represents the relative inclination angle  $I_{12}$  between the two planets (scale shown on the right axis). The nodal offset  $\Delta\Omega$  is librating with large amplitudes. The mutual inclination between the planetary orbits grows chaotically, inducing the large-amplitude eccentricity oscillations to the inner planet.

angular momentum vector  $\mathbf{L}_1$  is a superposition of two different motions, namely (i) the precession around the binary angular momentum vector  $\mathbf{L}_B$ , and (ii) the precession around the outer planet’s angular momentum vector  $\mathbf{L}_2$ . The resultant motion of  $\mathbf{L}_1$  is similar to the nutation of the spin axis of a gyroscope. When the gravitational attraction from the outer planet’s orbit is not sufficiently strong,  $\mathbf{L}_1$  and  $\mathbf{L}_2$  can grow a significantly large mutual inclination angle  $I_{12}$  (corresponds to the width of the cone shape that  $\mathbf{L}_1$  sweeps around  $\mathbf{L}_2$ ), as is the case for the example in Figure 8. The significant growth of the mutual inclination  $I_{12}$  induces additional Kozai cycles to the inner planet. Each maximum of  $e_1$  coincides with the minimum of  $I_{12}$ , similar to the standard Kozai cycles (Figure 9). However, the amplitude of the induced eccentricity oscillation is not constant since the angular momentum of the perturber  $m_2$  is also varying due to the interaction with the stellar companion.

Figure 9 focuses on the first 7 Myr of Figure 8. At  $t = 0$  planets are in nearly coplanar, nodally aligned orbits. The outer planet’s ascending node starts to rotate in the plane of the binary due to the perturbation from the stellar companion. As the nodal offset  $\Delta\Omega$  between the planetary orbits starts to grow, due to the gravitational attraction from the outer planet the inner planet begins to accelerate its nodal precession. At the same time, the orbital inclination  $I_1$  of the inner planet begins to grow to conserve the component of its orbital angular momentum parallel to  $\mathbf{L}_B$ . Shortly before 2 Myr, the mutual inclination  $I_{12}$  between the planetary orbits reaches  $\sim 40^\circ$ .

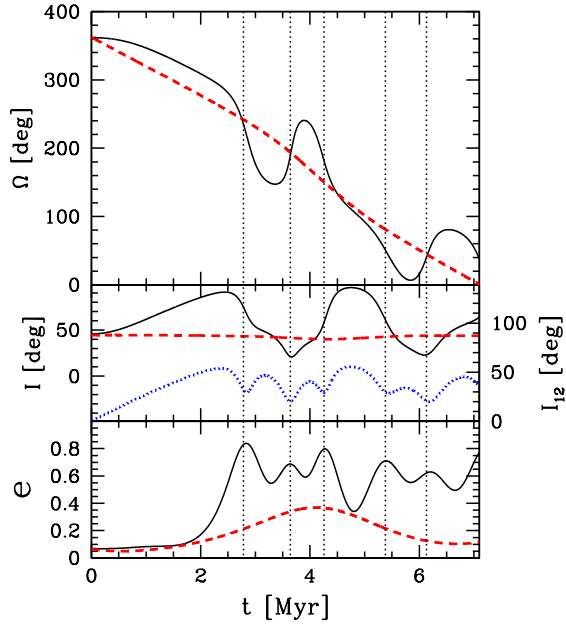


FIG. 9.— A close-in look of the first 7 Myr of Figure 8.

This initiates the Kozai cycles of the inner planet, and  $e_1$  starts to grow. At  $t \sim 2.5$  Myr the ascending nodes of the planets briefly return to alignment and  $e_1$  reaches the first maximum. At this moment, however, the planetary orbits are no longer perfectly coplanar because now the inner planet’s orbit has been further inclined with respect to the binary plane. The maximally accelerated nodal precession of the inner planet quickly passes ahead of the nodal line of the outer planet, thereby growing the mutual inclination and decreasing the orbital eccentricity. When the two nodes are maximally separated around  $t \sim 3.3$  Myr, the inner planet’s nodal precession changes the direction, and  $e_1$  starts to grow again. At  $t \sim 3.6$  Myr the planetary orbits are again nodally aligned, completing one nodal libration cycle. The chaotic eccentricity oscillation of the inner planet ensues quasi-periodically, corresponding to half the nodal libration period of the system estimated from the L-L theory,  $\tau_{\Omega_{pp}}/2 \approx 2$  Myr.

We make an additional comment on the effect of the GR precession on the evolution of the inner planet seen in Figure 8. During the sequence  $t = 8$ –14 Myr,  $e_1$  evolves non-periodically, which was not seen in a separate simulation of the same system without the GR effect. Notice that the pericenter argument  $\omega_1$  of the inner planet departs from the anti-alignment with  $\omega_2$  of the outer planet at  $t \sim 8$  Myr as the GR precession accelerates the precession of  $\omega_1$  toward apsidal alignment. During this epoch of the aligned apsidal libration, the induced Kozai cycles on the inner planet are suppressed. After  $t \sim 15$  Myr, the system returns to apsidal anti-alignment, and the chaotic oscillations of  $e_1$  resumes.

The chaotic eccentricity oscillation of the inner planet results from the stellar companion introducing a difference in the nodal precession frequencies between the planets. As previously mentioned in § 2.1, the nodal precession of the outer planet naturally follows from the secular three-body interactions with the binary stars and thus does not require the critical Kozai angle. In the

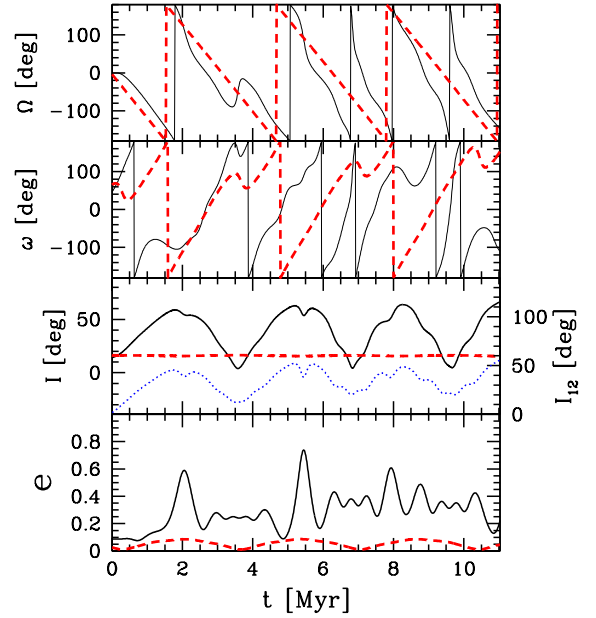


FIG. 10.— Large-amplitude eccentricity oscillations induced to the inner planet of a double-planet system with initial orbital inclination below the Kozai limit  $I_{\text{koz}}$ . The initial orbital parameters of the system are: for the inner planet (solid black curve)  $m_1 = 0.02M_J$ ,  $a_1 = 0.52$  AU,  $e_1 = 0.09$  and  $I_1 = 14.6^\circ$ ; for the outer planet (dashed red curve)  $m_2 = 0.76M_J$ ,  $a_2 = 7.53$  AU,  $e_2 = 0.03$  and  $I_2 = 16.5^\circ$ ; and for the binary companion  $M_B = 0.32M_\odot$ ,  $a_B = 419$  AU and  $e_B = 0.81$ . Despite the initially small orbital inclination, the eccentricity of the inner planet still oscillates with large amplitudes due to the large mutual inclination angle introduced between the two planetary orbits, while the Kozai cycles on the outer planet is significantly suppressed.

sample system shown in Figure 10, the two planets are initially inclined by only  $\sim 15^\circ$  with respect to the plane of the binary, significantly below the critical Kozai angle. Nonetheless, the nodal precession forced on the outer planet’s orbit causes the large-amplitude nodal libration of the planets, leading to the periodic growth of the mutual inclination angle. The inner planet’s orbital eccentricity grows to as large as  $e_1 \sim 0.8$  while the eccentricity oscillation of the outer planet is significantly suppressed.

### 3.3. Dynamically Rigid Systems

The previous examples highlight the evolution of planetary systems in which the nodal precession rate of the inner planet  $\dot{\Omega}_1$  is small compared to the nodal precession rate of the outer planet  $\dot{\Omega}_2$  induced by the stellar companion. Here we turn our attention to the regime  $\dot{\Omega}_1 > \dot{\Omega}_2$  so that the inner planet can effectively couple its nodal evolution to that of the outer planet, thereby maintaining a small mutual inclination angle.

Figure 11 illustrates the strong nodal coupling of planets. The inner Neptune-size planet ( $m_1 = 0.06M_J$ ) orbits at  $a_1 = 0.7$  AU, while the outer giant planet ( $m_2 = 0.22M_J$ ) orbits at  $a_2 = 9.1$  AU. The nodal precession timescale of the outer planet is  $\sim 2\tau_{\text{koz},2} = 20$  Myr. The secular nodal precession timescale of the inner planet can be estimated from the L-L theory and is smaller,  $\tau_{\Omega_{pp}} \sim 7$  Myr. As a result the inner planet successfully follows the nodal precession of the outer planet, maintaining tight nodal alignment and thus also a small mu-

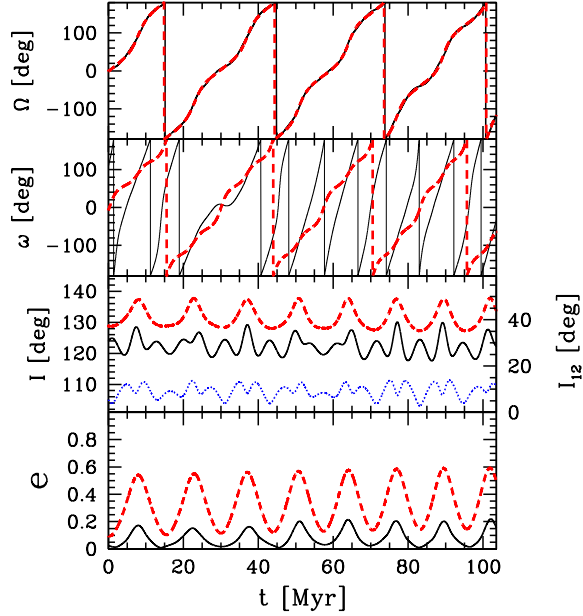


FIG. 11.— Evolution of a dynamically rigid double-planet system in a binary. The initial orbital parameters of the system are: for the inner planet (black solid curve)  $m_1 = 0.06M_J$ ,  $a_1 = 0.7$  AU,  $e_1 = 0.02$  and  $I_1 = 124^\circ$ ; for the outer planet (red dashed curve)  $m_2 = 0.22M_J$ ,  $a_2 = 9.1$  AU,  $e_2 = 0.09$  and  $I_2 = 129^\circ$ ; and for the binary companion  $M_B = 0.93M_\odot$ ,  $a_B = 952$  AU and  $e_B = 0.53$ . The blue dotted curve shows the relative inclination angle  $I_{12}$  between the two planets (scale shown on the right axis). In this system the ascending nodes of the planets are strongly coupled, and the system remains nearly coplanar. The pericenter arguments of the planets align briefly near the eccentricity maxima of the outer planet, resulting in the synchronous eccentricity oscillations of the planets.

tual inclination angle. Viewed from the orbital plane of the binary, the planetary orbits precess in concert, as if they were embedded in a rigid disk. We call such systems that rigidly respond to external perturbations “dynamically rigid” systems.

As seen in Figure 11, even though the dynamically-rigid planetary orbits remain nearly coplanar, the orbital eccentricity of the inner planet is still periodically excited. In this particular system the inner planet’s eccentricity oscillation is coupled to the Kozai cycles of the outer planet due to the periodic apsidal capture. The evolution of the same system in the  $e_2/e_1 - \Delta\omega$  space is presented in Figure 12. The contours with small dots are the secular trajectories analytically derived from the L-L theory. Without the presence of external perturbations, the planetary system would evolve on one of the secular trajectories selected from the initial conditions.

The planetary system is initially placed in the secular-circulation region,  $(e_2/e_1)_{\text{initial}} = 4.5$  and  $\Delta\omega_{\text{initial}} = -117^\circ$ . As the apsidal offset  $\Delta\omega$  between the planets circulates for  $360^\circ$  taking  $\tau_{\text{pp},1} \approx 7$  Myr, the system also shifts rightward in the diagram to new circulation contours due to the eccentricity growth of the outer planet (and thus growing  $e_2/e_1$ ) on a timescale  $\tau_{\text{koz},2} \approx 20$  Myr. Note that the contours to the right of the phase space are progressively more concentrated near the apsidal alignment  $\Delta\omega \sim 0^\circ$ . This is because the inner planet’s pericenter precesses much faster when its orbital eccentricity

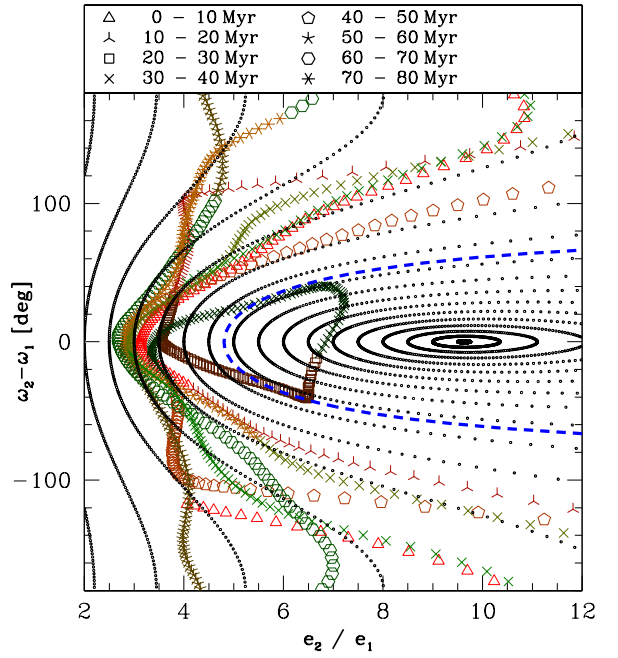


FIG. 12.— Orbital evolution of the planetary system from Figure 11, presented in the  $e_2/e_1 - \Delta\omega$  space. The small dots are the secular trajectories, and the blue dashed line is the secular separatrix dividing the regions of libration and circulation, both derived from the L-L theory. Different symbols are used to represent the different evolutionary stages of the system computed from numerical integration, with each symbol separated by  $10^5$  yr. The system spends a large fraction of time in the region of near apsidal-alignment (small  $\Delta\omega$ ), where the eccentricity ratio  $e_2/e_1$  of the planets is nearly fixed. During  $t \sim 20$ –40 Myr, the system briefly remains in the apsidal libration regime.

is smaller ( $e_2/e_1$  greater). Since the eccentricity ratio  $e_2/e_1$  is roughly fixed to a factor of a few around the apsidal alignment, at each episode of apsidal alignment the orbital eccentricity of the inner planet is excited. Notice that the eccentricity excitation timescale of the inner planet is significantly shortened by the outer planet bridging the angular momentum exchange from the stellar companion. Without the presence of the outer planet, the eccentricity excitation from the stellar companion occurs on a timescale  $\sim 1$  Gyr and thus would be completely suppressed by the GR precession. With the outer planet aiding the angular momentum exchange between the companion star and the inner planet, however, the inner planet can evolve on only  $\sim 20$  Myr, the timescale of the outer Kozai cycles.

This periodic apsidal-capture mechanism requires the dynamical rigidity of the system and a sufficiently large eccentricity oscillation amplitude of the outer planet, as well as comparable apsidal precession rates of the planets. The sample system shown in Figure 13 does not satisfy the last two of these conditions and thus fails to excite the inner planet’s eccentricity. First, in this example the two competing secular perturbations from the inner planet and from the stellar companion both precess the outer planet’s orbit in  $\sim 20$  Myr. As a result, the outer planet’s Kozai cycles are suppressed; its eccentricity reaches only as high as  $\sim 0.25$  while the maximum eccentricity predicted from the initial inclination is 0.58. Also, the apsidal precession timescale for the inner

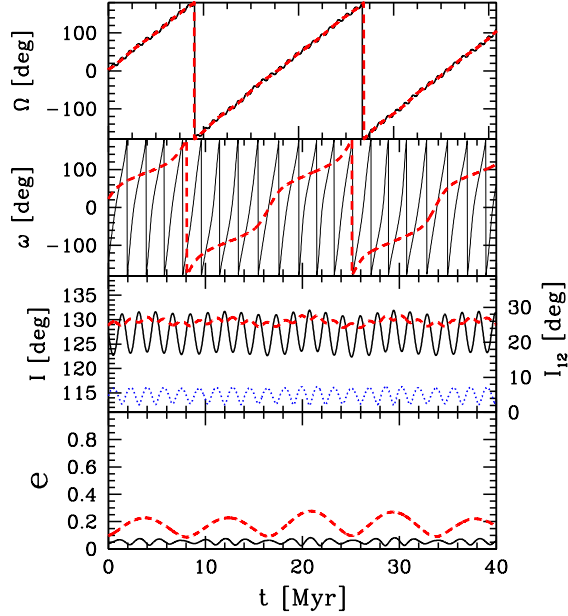


FIG. 13.— A dynamically-rigid planetary system with decoupled eccentricity evolutions. The initial orbital parameters of the system are: for the inner planet (black solid curve),  $m_1 = 0.75M_J$ ,  $a_1 = 1.15$  AU,  $e_1 = 0.04$  and  $I_1 = 127^\circ$ ; for the outer planet (red dashed curve),  $m_2 = 1.80M_J$ ,  $a_2 = 15.1$  AU,  $e_2 = 0.10$  and  $I_2 = 129^\circ$ ; for the binary companion,  $M_B = 0.80M_\odot$ ,  $a_B = 1322$  AU and  $e_B = 0.72$ . The secular torques are applied to the outer planet by the inner planet and also by the stellar companion at similar rates, thereby suppressing the amplitude of the outer planet’s eccentricity oscillation. The inner planet’s pericenter argument precesses  $\sim 10$  times as fast as that of the outer planet, prohibiting the capture into apsidal alignment. Consequently, the inner planet’s orbital eccentricity remains small throughout the evolution.

planet is  $\tau \sim 2$  Myr, much shorter than that of the outer planet,  $\tau \sim 20$  Myr, making the episodes of apsidal alignment too brief for the inner planet to adjust its orbital eccentricity.

In an opposite case in which the two apsidal frequencies are comparable within a factor of a few, the orbital eccentricity of the inner planet can be significantly altered at each maximum of the outer planet’s Kozai cycles. In Figure 14,  $\omega_1$  and  $\omega_2$  precess due to the outer planet and the stellar companion, respectively, both on timescales of a few Myr. These similar apsidal precession frequencies allow the long-lasting tight apsidal alignment of the planets during each Kozai cycle of the outer planet. Analogous to the example in Figure 12, as  $e_2$  begins to rise in the first 2 Myr, the growing eccentricity ratio  $e_2/e_1$  places the system on one of the more elongated circulation contours, on which the system quickly returns to the small value of  $e_2/e_1$  thereby steeply exciting  $e_1$  at the first Kozai maximum. When the outer planet’s eccentricity begins to decrease, it occurs on a timescale comparable to the circulation timescale of  $\omega_1$ , thus the inner planet does not have enough time to adjust to the circularization of the outer planet. Consequently, the eccentricity ratio  $e_2/e_1$  steadily drops to small values. When the outer planet completes its first Kozai cycle, the eccentricity ratio is inverted. For the first few Kozai cycles  $e_1$  is more effectively excited than damped, and it systematically drifts toward larger values. At the beginning of the fifth Kozai cycle of the outer planet ( $t \sim 11$  Myr), however,  $e_2/e_1$  has

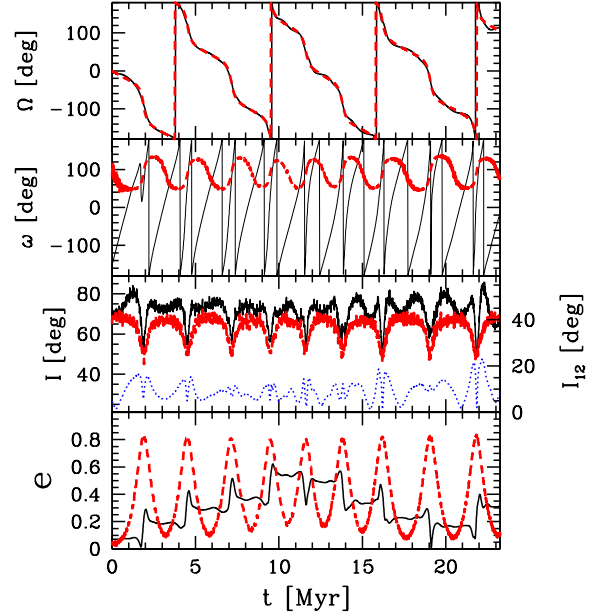


FIG. 14.— Evolution of a dynamically rigid planetary system in near secular apsidal resonance. The initial orbital parameters of the system are: for the inner planet (black solid curve),  $m_1 = 1.7M_J$ ,  $a_1 = 0.7$  AU,  $e_1 = 0.07$  and  $I_1 = 68^\circ$ ; for the outer planet (red dashed curve),  $m_2 = 4.5M_J$ ,  $a_2 = 16.4$  AU,  $e_2 = 0.03$  and  $I_2 = 65^\circ$ ; and for the binary companion,  $M_B = 0.4M_\odot$ ,  $a_B = 553$  AU and  $e_B = 0.37$ . The pericenter arguments of the two planets evolve on similar timescales. At every Kozai cycle of the outer planet, the pericenter of the inner planet is strongly captured into alignment or anti-alignment with the outer planet, resulting in impulsive excitation or damping of  $e_1$ .

been significantly reduced so that the inner planet gets captured into tight apsidal anti-alignment rather than alignment (see Eq. 26). During the anti-alignment the secular torque from the outer planet transfers angular momentum to the inner planet’s orbit which in turn reduces  $e_1$ . Consequently, the inner planet’s eccentricity secularly drifts between 0 and  $\sim 0.6$  as seen in Figure 14.

#### 4. DISCUSSION

##### 4.1. Analytical Boundaries of the Dynamical Classes of Planets in Binaries

The analytical boundaries in the parameter space of double-planet systems in binaries distinguishing each dynamical class presented in the previous section can be provided by comparing the several competing secular perturbation timescales of the systems. The L-L theory yields three eigenfrequencies that can be translated into orbital evolution timescales  $\tau_{pp,1}$ ,  $\tau_{pp,2}$ , and  $\tau_{\Omega pp}$ . For a pair of planets with a sufficiently large mass or semi-major axis ratio such that the outer Kozai cycles are not suppressed,  $\tau_{pp,1}$  and  $\tau_{pp,2}$  are approximated to the apsidal precession timescales of the inner and the outer planets, respectively, and  $\tau_{\Omega pp}$  corresponds to the characteristic nodal precession timescale of the planets. A stellar companion also secularly perturbs the inner and the outer planet on timescales  $\tau_{koz,1}$  and  $\tau_{koz,2}$ , respectively. Figure 15 shows that, generally, for a large region of the parameter space  $\tau_{pp,1} < \tau_{koz,1}$ , a regime in which the inner planet’s evolution is affected only by the outer planet. For the outer planet, the condition we have im-

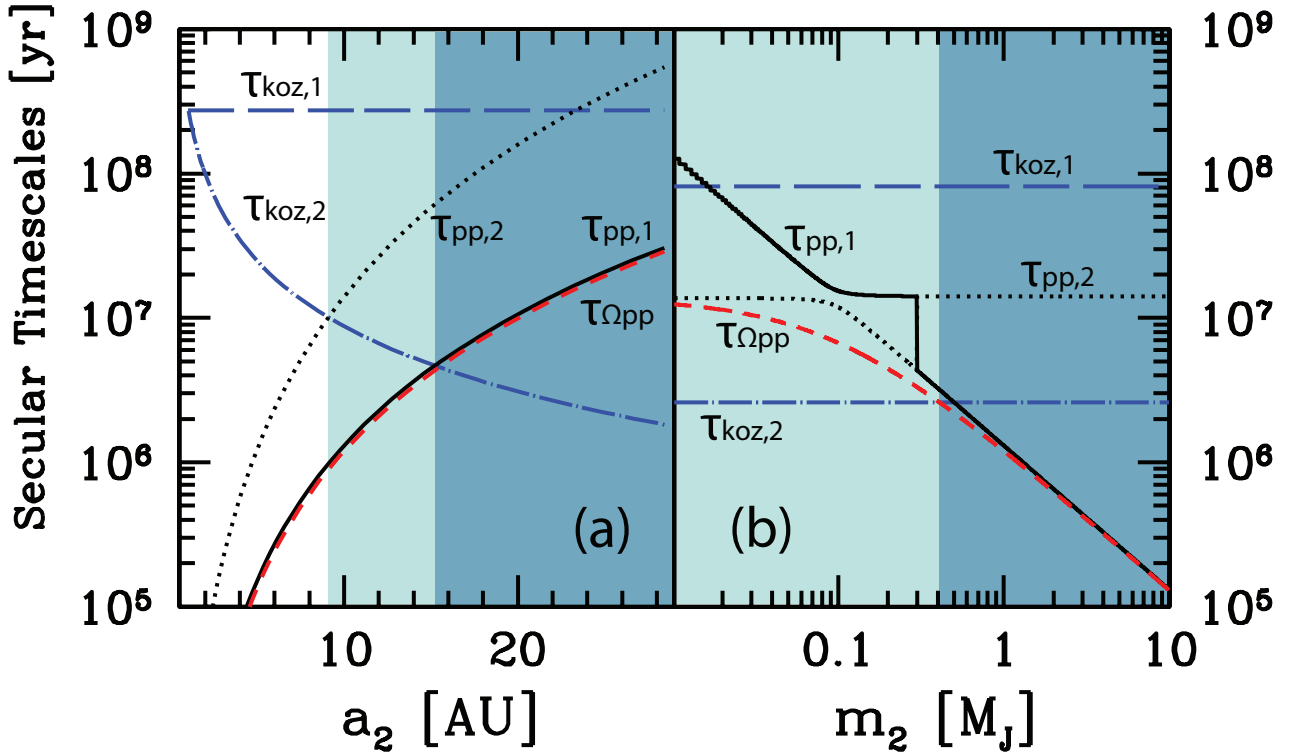


FIG. 15.— Various secular timescales of double planets in a binary as a function of (a) the orbital semi-major axis and (b) the mass of the outer planet, with the following system parameters :  $m_1 = 0.3M_J$ ,  $a_1 = 1 \text{ AU}$ ,  $m_B = 1M_\odot$ ,  $a_B = 500 \text{ AU}$ , and  $e_B = 0.5$ . In the left panel (a)  $m_2 = 1M_J$ , and in the right panel (b)  $a_2 = 10 \text{ AU}$ . In the unshaded area, the Kozai cycles on the outer planet would be suppressed by the secular torque from the inner planet. In the light-shaded region, planetary systems undergo dynamically-rigid evolution. In the dark-shaded region, the orbital eccentricity of the inner planet grows chaotically due to the growing mutual inclination between the planetary orbits.

posed is such that the perturbation from the stellar companion overcomes the perturbation from the inner planet, i.e.,  $\tau_{pp,2} > \tau_{koz,2}$ , typically corresponding to relatively hierarchical systems (the shaded regions in Figure 15).

For such hierarchical systems in which the stellar companion secularly perturbs the outer planet’s orbit, two distinctively different evolutionary processes are possible, depending on whether the planets can rigidly respond to the quadrupole perturbations from the stellar companion, maintaining a small mutual inclination angle  $I_{12}$ . The key quantity which separates the two dynamical classes is the nodal precession rate of each planet. The ascending node of the outer planet secularly precesses due to the binary companion roughly on a timescale  $2\tau_{koz,2}$ . The nodal-coupling strength of the inner planet to the outer planet can be quantified by the nodal precession timescale  $\tau_{\Omega pp}$  derived from the L-L theory. If the outer planet’s nodal precession occurs faster than that of the inner planet such that

$$\tau_{\Omega pp} > 2\tau_{koz,2}, \quad (31)$$

corresponding to the darker-shaded region of Figure 15, then a large mutual inclination angle opens between the planetary orbits, and the additional Kozai cycles are induced to the inner planet on a timescale  $\tau_{ind,Koz}$  which is shorter than the timescale  $\tau_{koz,1}$  of a direct perturbation from the stellar companion,

$$\tau_{ind,Koz} \sim \frac{2}{3} \frac{P_2^2}{P_1} \frac{m_0}{m_2} < \tau_{koz,2} < \tau_{koz,1}. \quad (32)$$

The amplitude of the induced eccentricity oscillation is not constant because the Kozai integral of the inner

planet measured in the frame of the outer planet’s orbit does not remain constant as the outer planet is also subject to angular momentum exchange with the stellar companion.

If, on the other hand, the gravitational nodal coupling between the planetary orbits is comparably strong such that the nodal precession of the inner planet does not lag significantly behind that of the outer planet, i.e.,

$$\tau_{\Omega pp} < 2\tau_{koz,2}, \quad (33)$$

then the planetary orbits can remain close to coplanar.

In dynamically rigid planetary systems the orbital eccentricity of the inner planet may still evolve, depending on the strength of the apsidal coupling between the planets. The most extreme case is when the two apsidal frequencies are close to the secular resonance such that

$$\tau_{pp,1} \sim \tau_{koz,2}. \quad (34)$$

In such cases, the inner planet gets periodically trapped into apsidal alignment or anti-alignment with the outer planet. Such repeated apsidal coupling is responsible for the secularly-drifting orbital eccentricity of the inner planet illustrated in Figure 14. When the pericenter evolution of the planets is less strongly coupled, the orbital eccentricity of the inner planet is periodically excited synchronously with the outer Kozai cycles (Figure 11). If the coupling further weakens such that

$$\tau_{pp,1} \ll \tau_{koz,2}, \quad (35)$$

then the two apsidal precessions are completely independent, and the inner planet’s eccentricity remains small (Figure 13).

#### 4.2. Stability of Planets in Binaries

A stellar companion may induce instability to the double-planet system around the primary star that can otherwise remain stable for a long term. A possible trigger of instability is either the Kozai cycles of the outer planet, or the chaotic eccentricity oscillation induced to the inner planet. In both cases what may follow is the loss of a planet either through collision with the host star or ejection from the system. The first case of instability is rarely observed in our simulations because we have imposed the Hill stability criterion on the initial conditions, including the predicted maximum orbital eccentricity of the outer planet. The majority of the unstable outcomes are found in systems with additional Kozai cycles induced to the inner planet due to the broken coplanarity between the planetary orbits. It needs to be remembered, however, that our simulations do not include any orbital damping mechanism such as tidal dissipation effects. Because the eccentricity growth of the inner planet induced by the outer planet is rather adiabatic than impulsive, were tidal effects included in the simulations, many of these highly eccentric planets would effectively damp their orbital eccentricities and migrate to tighter orbits before being lost from the system.

### 5. SUMMARY

We have shown that the complex interplay between the secular gravitational perturbations from a stellar companion and the gravitational coupling between planets produces various classes of dynamical outcomes. The two distinct evolutionary processes are the dynamically-rigid evolution of planetary orbits, and the chaotic growth of the mutual inclination angle between the planets. The dynamical rigidity of planetary systems can be analytically estimated by comparing the nodal precession rates of the planets. A weak nodal coupling between the planets such that  $\tau_{\Omega_{pp}} > \tau_{\text{koz},2}$  leads to large-amplitude nodal libration which steeply inclines the orbital plane of the inner planet with respect to the outer planet. Consequently, the inner planet suffers secular eccentricity oscillation with chaotically varying amplitudes. If, on the other hand, the gravitational nodal coupling of the planets is stronger than the nodal perturbation to the outer planet caused by the stellar companion such that  $\tau_{\Omega_{pp}} < \tau_{\text{koz},2}$ , then the orbital planes of the planets precess in concert, maintaining near-coplanarity. Even in dynamically-rigid planetary systems, the orbital eccentricity of the inner planet can remain small, or periodically excited in response to the outer Kozai cycles, or secularly drift within a large range, depending on the apsidal precession frequencies of the planets.

The periodic eccentricity and inclination perturbations from a stellar companion propagating inward through the planetary system effectively reduces the orbital evolution timescale of the inner planet. Such a cascading angular momentum transfer mechanism needs to be incorporated to the existing theoretical models of extrasolar planetary systems in binaries. The traditionally adopted constraint of the critical Kozai angle between the planetary systems and the binary orbits may be even relaxed, if undetected, non-coplanar planetary companions are applying eccentricity perturbations to the detected ones. Figure 15 indicates that there is a threshold for the orbital radius of the outer planet beyond which the induced Kozai cycles

of the inner planet are almost certain ( $a_2 \gtrsim 15$  AU for the system presented in Figure 15). Also, in a less hierarchical system with ensured dynamical rigidity ( $a_2 \sim 10$ – $15$  AU in Figure 15), the inner planet’s eccentricity can be still excited given suitable apsidal-capture conditions. Thus, the eccentricity excitation of extrasolar planets by binary perturbations is possibly much more efficient than previously predicted in the studies based on single-planet assumptions (Takeda & Rasio 2005).

In this paper we have provided a general dynamical framework for understanding planetary systems in binaries. Yet, there remain some limitations in our study which will be further investigated in our future papers. First, a broader range of initial planetary eccentricities and inclinations needs to be considered. Recent theoretical studies have shown that newly-formed planets emerging from a protoplanetary disk may already possess large orbital eccentricities or inclinations because of interactions with the gaseous disk (Goldreich & Sari 2003; Moorhead & Adams 2007) or through planet–planet scattering events (Chatterjee et al. 2007; Juric & Tremaine 2007; Nagasawa et al. 2008). More realistic distributions of initial orbital parameters are necessary to accurately determine the likelihood of each dynamical class of planets in binaries presented here. Second, we have not included tidal dissipation, which may also affect the dynamical outcomes of planets in binaries. The orbital energy dissipation of highly eccentric planets through tidal friction and subsequent orbital migration have been previously studied for hierarchical three-body systems (Wu & Murray 2003; Fabrycky & Tremaine 2007; Wu et al. 2007). Since significant eccentricity growth of the inner planet naturally results when the coplanarity between planetary orbits is destroyed, the formation of close-in planets among multiple-planet systems in binaries through tidal dissipation may be fairly common.

As the observational techniques continue to advance, direct measurements of the following observable signatures will be possible to constrain the dynamical outcomes of planets in binaries: (1) the mutual inclination angle among multiple-planet systems in binaries measured by astrometric observations (e.g., the preliminary results for *v* Andromedae system by HST Fine Guiding Sensor show a large mutual inclination angle  $\sim 35^\circ$  between the planets c and d; McArthur et al. 2007); (2) large spin-orbit misalignments of close-in transiting planets possibly formed via induced Kozai migration, measured through the Rossiter-McLaughlin effect (Fabrycky & Tremaine 2007); (3) detections of additional planets beyond a few AU from the primary stars of binary systems by continuous radial-velocity monitoring of known planetary systems; (4) detections of stellar companions around known hierarchical multiple-planet systems by ongoing co-proper motion surveys.

This work was supported by NSF Grant AST-0507727. We are grateful to Lamya Saleh for providing us an improved version of the Mercury BS integrator including the lowest-order post-Newtonian correction. We also thank Ji-Lin Zhou, Daniel Fabrycky, and Fred Adams for useful discussions.

## REFERENCES

- Artymowicz, P. & Lubow, S. H. 1994, *ApJ*, 421, 651  
 Brouwer, D. & Clemence, G. M. 1961, *Methods of celestial mechanics* (New York: Academic Press, 1961)  
 Chambers, J. E. 1999, *MNRAS*, 304, 793  
 Chatterjee, S., Ford, E. B., & Rasio, F. A. 2007, *ArXiv Astrophysics e-prints*  
 Chiang, E. I. & Murray, N. 2002, *ApJ*, 576, 473  
 Desidera, S. & Barbieri, M. 2007, *A&A*, 462, 345  
 Eggenberger, A., Udry, S., Chauvin, G., Beuzit, J.-L., Lagrange, A.-M., Ségransan, D., & Mayor, M. 2007, *A&A*, 474, 273  
 Eggenberger, A., Udry, S., & Mayor, M. 2004, *A&A*, 417, 353  
 Fabrycky, D. & Tremaine, S. 2007, *ArXiv e-prints*, 705  
 Ford, E. B., Kozinsky, B., & Rasio, F. A. 2000, *ApJ*, 535, 385  
 Ford, E. B., Lystad, V., & Rasio, F. A. 2005, *Nature*, 434, 873  
 Gladman, B. 1993, *Icarus*, 106, 247  
 Goldreich, P. & Sari, R. 2003, *ApJ*, 585, 1024  
 Hale, A. 1994, *AJ*, 107, 306  
 Harrington, R. S. 1968, *AJ*, 73, 190  
 Holman, M., Touma, J., & Tremaine, S. 1997, *Nature*, 386, 254  
 Ida, S. & Lin, D. N. C. 2005, *ApJ*, 626, 1045  
 Innanen, K. A., Zheng, J. Q., Mikkola, S., & Valtonen, M. J. 1997, *AJ*, 113, 1915  
 Juric, M. & Tremaine, S. 2007, *ArXiv Astrophysics e-prints*  
 Kinoshita, H. & Nakai, H. 1999, *Celestial Mechanics and Dynamical Astronomy*, 75, 125  
 Kiseleva, L. G., Eggleton, P. P., & Mikkola, S. 1998, *MNRAS*, 300, 292  
 Kley, W. & Nelson, R. 2007, *ArXiv e-prints*, 705  
 Kozai, Y. 1962, *AJ*, 67, 591  
 Lee, M. H. & Peale, S. J. 2003, *ApJ*, 592, 1201  
 Malhotra, R. 2002, *ApJ*, 575, L33  
 Malmberg, D., Davies, M. B., & Chambers, J. E. 2007, *MNRAS*, 377, L1  
 Marzari, F., Scholl, H., & Tricarico, P. 2005, *A&A*, 442, 359  
 Mayer, L., Wadsley, J., Quinn, T., & Stadel, J. 2005, *MNRAS*, 363, 641  
 McArthur, B., Benedict, G. F., Bean, J., & Martioli, E. 2007, in *American Astronomical Society Meeting Abstracts*, Vol. 211, American Astronomical Society Meeting Abstracts, 134.17+  
 Moorhead, A. V. & Adams, F. C. 2007, *ArXiv e-prints*, 708  
 Murray, C. D. & Dermott, S. F. 1999, *Solar system dynamics* (Solar system dynamics by Murray, C. D., 1999)  
 Nagasawa, M., Ida, S., & Bessho, T. 2008, *ArXiv e-prints*, 801  
 Nelson, A. F. 2000, *ApJ*, 537, L65  
 Pichardo, B., Sparke, L. S., & Aguilar, L. A. 2005, *MNRAS*, 359, 521  
 Raghavan, D., Henry, T. J., Mason, B. D., Subasavage, J. P., Jao, W.-C., Beaulieu, T. D., & Hambly, N. C. 2006, *ApJ*, 646, 523  
 Takeda, G. & Rasio, F. A. 2005, *ApJ*, 627, 1001  
 Thommes, E. W., Bryden, G., Wu, Y., & Rasio, F. A. 2007, *ArXiv e-prints*, 706  
 Udry, S. & Santos, N. C. 2007, *ARA&A*, 45, 397  
 Valenti, J. A. & Fischer, D. A. 2005, *ApJS*, 159, 141  
 Veras, D. & Armitage, P. J. 2007, *ApJ*, 661, 1311  
 Wu, Y. & Murray, N. 2003, *ApJ*, 589, 605  
 Wu, Y., Murray, N. W., & Ramsahai, J. M. 2007, *ApJ*, 670, 820  
 Zhou, J.-L. & Sun, Y.-S. 2003, *ApJ*, 598, 1290  
 Zhou, J.-L. & Sun, Y.-S. 2004, in *IAU Symposium*, Vol. 219, *Stars as Suns : Activity, Evolution and Planets*, ed. A. K. Dupree & A. O. Benz, 820+  
 Zucker, S. & Mazeh, T. 2002, *ApJ*, 568, L113